Future Medicinal Chemistry

ISSN: (Print) (Online) Journal homepage: www.tandfonline.com/journals/ifmc20

Biological, computational evaluation of novel benzofuranyl derivatives as acetylcholinesterase and butyrylcholinesterase

Hande Usanmaz, Ömer Taş, Deniz Ekinci, Abdullahi Ibrahim Uba & Ufuk Atmaca

To cite this article: Hande Usanmaz, Ömer Taş, Deniz Ekinci, Abdullahi Ibrahim Uba & Ufuk Atmaca (30 May 2024): Biological, computational evaluation of novel benzofuranyl derivatives as acetylcholinesterase and butyrylcholinesterase, Future Medicinal Chemistry, DOI: 10.1080/17568919.2024.2342641

To link to this article: https://doi.org/10.1080/17568919.2024.2342641

FUTURE MEDICINAL CHEMISTRY
https://doi.org/10.1080/17568919.2024.2342641

Taylor & Francis
Taylor & Francis Group

RESEARCH ARTICLE

Biological, computational evaluation of novel benzofuranyl derivatives as acetylcholinesterase and butyrylcholinesterase

Hande Usanmaz[a], Ömer Taş[b], Deniz Ekinci[b], Abdullahi Ibrahim Uba[c] and Ufuk Atmaca[*,d]

[a]Vocational School of Health Service, Medical Laboratory Techniques Program, Sinop University, Sinop, 57000, Turkey; [b]Faculty of Agriculture, Department of Agricultural Biotechnology, Ondokuz Mayıs University, Samsun, 55100, Turkey; [c]Department of Molecular Biology & Genetics, Istanbul AREL University, Istanbul, 34010, Turkey; [d]Department of Chemistry, Faculty of Sciences, Atatürk University, Erzurum, 25240, Turkey

ABSTRACT

Aim: A highly efficient one-step method has been developed for the synthesis of benzofuranyl derivatives from 2-benzoylcyclohexane-1-carboxylic acid derivatives using chlorosulfonyl isocyanate. This novel method provides a practical, cost-effective and efficient approach. **Materials & methods:** The inhibitory effects of benzofuranyl derivatives on acetylcholinesterase (AChE) and butyrylcholinesterase (BChE) enzymes were investigated. Ki values were determined to range from 0.009 to 0.61 μM for AChE and 0.28 to 1.60 μM for BChE. Molecular docking analysis provided insights into the interaction modes and binding patterns of these compounds with AChE and BChE. **Conclusion:** Kinetic findings of our study suggest that some of our compounds exhibited more effective low micromolar inhibition compared with the reference, and these derivatives could be to design more powerful agents.

ARTICLE HISTORY
Received 13 January 2024
Accepted 4 April 2024

KEYWORDS
acetylcholinesterase; Alzheimer's disease; benzofuranyl; butyrylcholinesterase; molecular modeling

1. Background

Cholinesterases are a group of enzymes found in organisms that play important roles in the body. Choline, a compound with significant functions in the body, is regulated by cholinesterases, which are present in the brain, muscles, nervous system and other tissues [1]. Among others, acetylcholinesterase (AChE) and butyrylcholinesterase (BChE), are the best-known cholinesterase enzymes.

AChE, present in the nervous system, terminates the action of a neurotransmitter called acetylcholine. Acetylcholine is a compound used for communication between nerve cells, and AChE breaks down acetylcholine molecules, rendering them inactive. In this way, it ensures the proper control of nerve transmission [2]. The breakdown of acetylcholine through cholinesterases completes nerve transmission after its release from cholinergic synapses [3].

Choline is a component of phosphatidylcholine, a phospholipid that makes up the structure of cell membranes. BChE recycles choline by breaking down choline esters, contributing to the maintenance of cell membrane structure and function. BChE also breaks down acetylcholine, contributing to the regulation of nerve signals [4]. Certain anesthesia drugs are metabolized by BChE, which contributes to the termination of their effects and is important in controlling the effects of these drugs [5].

AChE inhibitors inhibit the action of acetylcholinesterase but do not inhibit butyrylcholinesterase. BChE performs the hydrolysis of various ester derivatives [6]. Alzheimer's disease affects cognitive functions, including memory and thinking abilities. It has seen a significant increase in developed countries due to the aging population [7,8]. Many researches have demonstrated that the activity of BChE and AChE change in Alzheimer's disease [9]. Acetylcholinesterase inhibitors are used to treat cognitive symptoms of neurodegenerative circumstances such as Alzheimer's disease, Parkinson's disease, Lewy body dementia and dementia. Additionally, inhibitors of AChE have the potential to be used in the treatment of disorders like autism [10].

Benzofuranyl groups are useful scaffolds that possess desirable bioactive properties [11,12]. The benzofuranyl moiety serves as an important part of natural products (e.g., digitoxin, (-)-incrustoporin, plumieride, patulin) and a series of pharmacologically active compounds (rofecoxib, digoxin, protoanemonin) (Figure 1A) [13,14]. These molecules exhibits wide spectrum of biological activities such as antibacterial, antifungal, antitumor, insecticides and neurotoxicity [15–20]. Therefore, a practical, mild and effective route is highly desirable for the synthesis of α,β-

CONTACT Ufuk Atmaca uatmaca@atauni.edu.tr

Supplemental data for this article can be accessed at https://doi.org/10.1080/17568919.2024.2342641

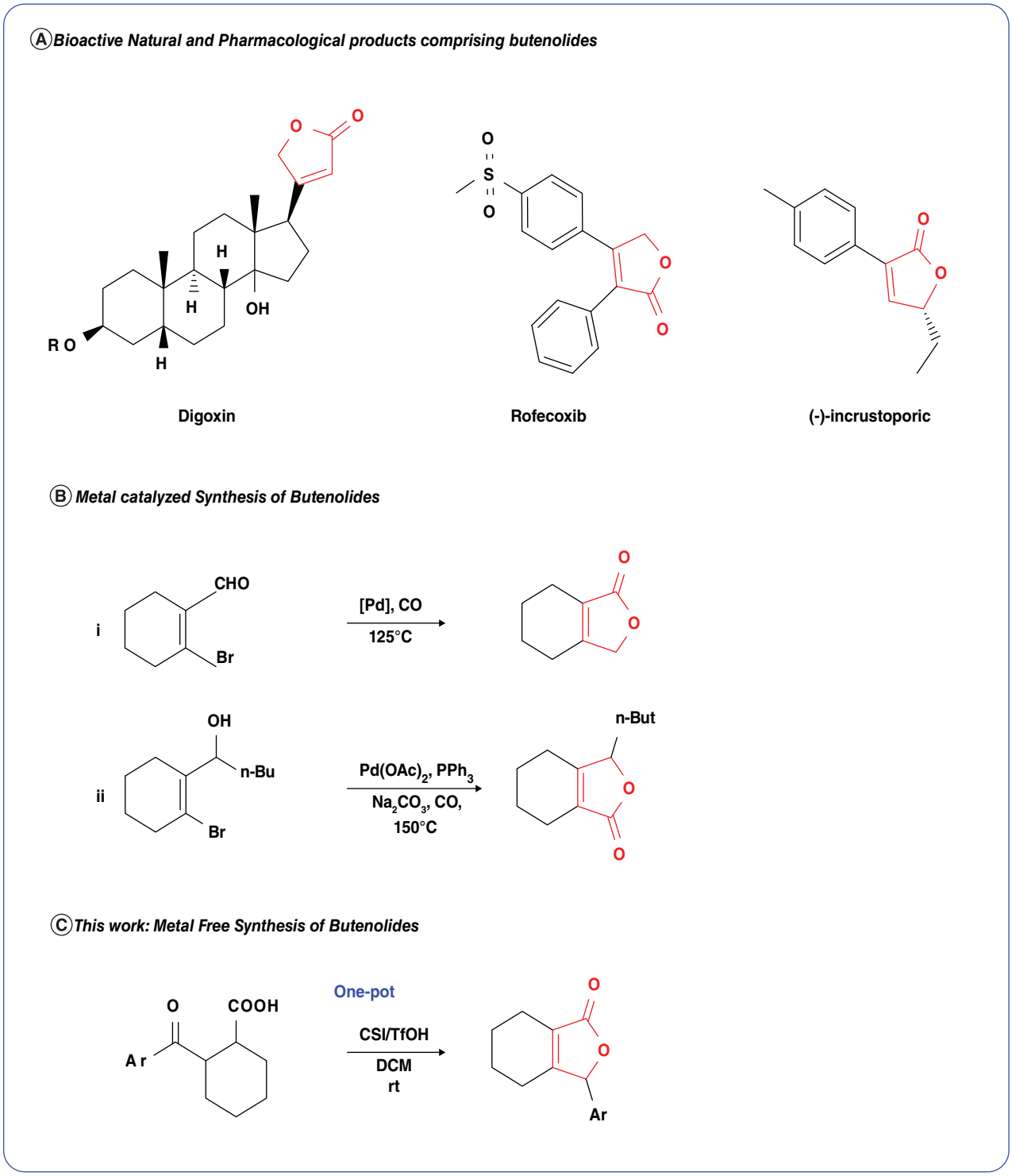

Figure 1. Research background of benzofuranyl derivatives. **(A)** Bioactive natural and pharmacological products comprising butenolides. **(B)** Metal catalyzed synthesis of butenolides. **(C)** This work: metal-free synthesis of butenolides

unsaturated lactones. For the first time, all new molecules have been synthesized racemically.

The syntheses of benzofuranyl were reported from β-Bromovinyl aldehydes reacting with alcohols and carbon monoxide at 125°C in 66% yields via palladium-catalyzed (Figure 1B-i) [21], and from carbonylative cyclization of 3-bromoallyl alcohols via palladium-catalyzed (Figure 1B-ii) [22]. However, the pharmaceutical industry and organic syntheses have disadvantages such as hard conditions, high reaction temperatures, long reaction times and the use of metal catalysis. We recently published the use of chlorosulfonyl isocyanate (CSI) as a versatile reagent

in organic synthesis [23–25]. Here we report a practical, novel, synthesis of benzofuranyl groups via intramolecular cyclization with chlorosulfonyl isocyanate without any metal catalysts in good yields and under mild conditions (Figure 1C) Here we report the *in vitro* inhibition activities of these benzofuranyl derivatives on AChE and BuChE enzymes.

2. Experimental

2.1. General remarks

Solvents, hexahydroisobenzofuran-1,3-dione and CSI were commercially available. 2-benzoylcyclohexane-1-carboxylic acid and their derivatives (**1a–j**) were synthesized with Friedel-Crafts Acylation as stated in the literature [26]. IR spectra were obtained from solutions in 0.1 mm cells and in CH_2Cl_2 with a Perkin-Elmer spectrophotometer (MA, USA). ^{1}H-NMR and ^{13}C-NMR spectra were recorded on a Bruker spectrometers (MA, USA) at 400 and 100 MHz, respectively, and NMR shifts are presented as δ in ppm. Melting points were recorded on a melting-point apparatus (Gallenkamp, Canada; WA11373). All docking runs were performed using AutoDock 4.2.6 (https://autodock.scripts.edu) while adopting the docking protocol described in [27]. All protein–ligand visualization was done using Biovia DS Visualizer v4.5 (BIOVIA, CA, USA).

2.2. General procedure synthesis of benzofuranyl derivatives

CSI (1.1 eq) was added to a solution of 2-benzoylcyclohexane-1-carboxylic acid and their derivatives (**1a–j**) (1.0 eq) and a catalytic amount of TfOH (trifluorosulfonic acid) in 10 ml dichloromethane and stirred for 3 h at room temperature. After that, volatiles were evaporated under reduce pressure. TLC was used to purify the residue that resulted, and EtOAc:*n*-hexane (1:4) was used as the eluent to produce the pure product.

2.2.1. 3-Phenyl-4,5,6,7-tetrahydroisobenzofuran-1(3H)-one (2a)

Yellow liquid (86%); ^{1}H-NMR (400 MHz, $CDCl_3$, ppm) δ 7.35–7.39 (m, 3H), 7.19–7.22 (m, 4H), 5.69 (s, 1H), 2.27–2.30 (m, 2H), 2.18–2.24 (m, 1H), 1.92–1.98 (m, 1H), 1.63–1.78 (m, 4H); ^{13}C-NMR (100 MHz, $CDCl_3$, ppm) δ 19.9, 21.5(2C), 23.1, 84.6, 126.3, 126.5, 129.0, 129.1, 135.1, 163.9, 173.9; IR ($CHCl_3$, cm^{-1}): 3065, 2938, 1750, 1678, 1454, 1299, 1235, 1025; HRMS (ESI): calcd for $C_{14}H_{14}O_2$ [$(M+H)^+$]: 214.0994; found: 214.0990.

2.2.2. 3-(p-Tolyl)-4,5,6,7-tetrahydroisobenzofuran-1(3H)-one (2b)

Yellow liquid (88%); ^{1}H-NMR (400 MHz, $CDCl_3$, ppm) δ 7.17 (d, *J*: 8.1 Hz, 2H), 7.08 (d, *J*: 8.1 Hz, 2H), 5.66 (s, 1H), 2.35 (s, 3H), 2.27–2.29 (m, 2H), 2.16–2.22 (m, 1H), 1.98–2.03 (m, 1H), 1.64–1.76 (m, 4H); ^{13}C-NMR (100 MHz, $CDCl_3$, ppm) δ 20.0, 21.5, 21.6(2C), 23.1, 84.5, 125.9, 126.5, 129.6, 132.0, 139.1, 163.9, 173.9; IR ($CHCl_3$, cm^{-1}): 2936, 1754, 1677, 1515, 1448, 1391, 1300, 1235, 1113, 1028; HRMS (ESI): calcd for $C_{15}H_{16}O_2$ [$(M+H)^+$]: 228.1150; found: 218.1142.

2.2.3. 3-(4-ethylphenyl)-4,5,6,7-tetrahydroisobenzofuran-1(3H)-one (2c)

Yellow liquid (75%); ^{1}H-NMR (400 MHz, $CDCl_3$, ppm) δ 7.13 (d, *J*: 8.1 Hz, 2H), 7.04 (d, *J*: 8.1 Hz, 2H), 5.59 (s, 1H), 2.57 (q, *J*: 7,7 Hz, 2H), 2.22–2.24 (m, 2H), 2.09–2.17 (m, 1H), 1.87–1.97 (m, 1H), 1.57–1.71 (m, 4H), 1,16 (t, *J*: 7.7 Hz, 3H); ^{13}C-NMR (100 MHz, $CDCl_3$, ppm) δ 15.4, 20.0, 21.5, 21.6, 23.6, 28.6, 84.5, 126.1, 126.6, 128.4, 132.3, 145.3, 163.8, 173.8; IR ($CHCl_3$, cm^{-1}): 2931, 1753, 1678, 1390, 1297, 1107, 1027, 941; HRMS (ESI): calcd for $C_{16}H_{18}O_5$ [$(M+H)^+$]: 242.1307; found: 342.1325.

2.2.4. 3-(4-propylphenyl)-4,5,6,7-tetrahydroisobenzofuran-1(3H)-one (2d)

Yellow liquid (77%); ^{1}H-NMR (400 MHz, $CDCl_3$, ppm) δ 7.10 (d, *J*: 8.1 Hz, 2H), 7.02 (d, *J*: 8.1 Hz, 2H), 5.58 (s, 1H), 2.50 (t, *J*: 7,8 Hz, 2H), 2.19–2.21 (m, 2H), 2.08–2.17 (m, 1H), 1.86–1.91 (m, 1H), 1.50–1.69 (m, 6H), 0,87 (t, *J*: 7.8 Hz, 3H); ^{13}C-NMR (100 MHz, $CDCl_3$, ppm) δ 13.8, 19.9, 21.5, 21.6, 23.2, 24.4, 37.7, 84.5, 126.0, 126.5, 129.0, 132.3, 143.8, 163.8, 173.9; IR ($CHCl_3$, cm^{-1}): 2931, 2862, 1754, 1679, 1351, 1296, 1027; HRMS (ESI): calcd for $C_{17}H_{20}O_2$ [$(M+H)^+$]: 256.1463; found: 256.1472.

2.2.5. 3-(4-isopropylphenyl)-4,5,6,7-tetrahydroisobenzofuran-1(3H)-one (2e)

Yellow liquid (79%); ^{1}H-NMR (400 MHz, $CDCl_3$, ppm) δ 7.15 (d, *J*: 8.1 Hz, 2H), 7.04 (d, *J*: 8.1 Hz, 2H), 5.59 (s, 1H), 2,83 (septet, *J*: 6.9 Hz, 1H), 2.22–2.24 (m, 2H), 2.10–2.17 (m, 1H), 1.88–1.96 (m, 1H), 1.58–1.65 (m, 4H), 1.16 (d, *J*: 6.9 Hz, 6H); ^{13}C-NMR (100 MHz, $CDCl_3$, ppm) δ 20.0, 21.5, 21.6, 23.2, 23.9, 33.9, 84.5, 126.1, 126.6, 127.0, 132.4, 149.9, 163.7, 173.8; IR ($CHCl_3$, cm^{-1}): 2958, 1755, 1678, 1513, 1390, 1108, 1027; HRMS (ESI): calcd for $C_{17}H_{20}O_5$ [$(M+H)^+$]: 256.1463; 256.1455.

2.2.6. 3-(3,4-dimethylphenyl)-4,5,6,7-tetrahydroisobenzofuran-1(3H)-one (2f)

White solid (82%), m.p 92–94°C; ^{1}H-NMR (400 MHz, $CDCl_3$, ppm) δ 7.14 (d, *J*: 8.1 Hz, 1H), 6.93–6.96 (m, 2H), 5.64 (s, 1H), 2.30–2.32 (m, 2H), 2.27 (s, 6H), 2.18–2.25 (m, 1H), 1.96–2.02 (m, 1H), 1.66–1.78 (m, 4H); ^{13}C-NMR (100 MHz, $CDCl_3$,

ppm) δ 19.6, 19.8, 20.0, 21.5, 21.6, 23.1, 84.6, 124.1, 125.9, 127.6, 130.1, 132.4, 137.3, 137.7, 163.9, 173.9; IR ($CHCl_3$, cm^{-1}): 2928, 1757, 1677, 1449, 1389, 1298, 1106, 1026; HRMS (ESI): calcd for $C_{16}H_{18}O_2$ [$(M+H)^+$]: 242.1307; found: 242.1316.

2.2.7. 3-(2,5-dimethylphenyl)-4,5,6,7-tetrahydroiso benzofuran-1(3H)-one (2g)

White solid (84%), m.p 96–98°C; ^{1}H-NMR (400 MHz, $CDCl_3$, ppm) δ 7.05–7.12 (m, 2H), 6.80 (s, 1H), 5.98 (s, 1H), 2.38 (s, 3H), 2.31–2.36 (m, 2H), 2.29 (s, 3H), 2.20–2.27 (m, 1H), 2.01–2.07 (m, 1H), 1.67–1.80 (m, 4H); ^{13}C-NMR (100 MHz, $CDCl_3$, ppm) δ 18.8, 20.1, 21.0, 21.5, 21.6, 23.3, 81.7, 126.5, 126.7, 129.6, 130.9, 132.7, 133.1, 136.2, 163.9, 174.0; IR ($CHCl_3$, cm^{-1}): 2930, 1752, 1677, 1504, 1448, 1389, 1294, 1148, 1026; HRMS (ESI): calcd for $C_{16}H_{18}O_2$ [$(M+H)^+$]: 242.1307; found: 242.1304.

2.2.8. 3-(2,4-dimethylphenyl)-4,5,6,7-tetrahydroiso benzofuran-1(3H)-one (2h)

White solid (83%), m.p 99–101°C; ^{1}H-NMR (400 MHz, $CDCl_3$, ppm) δ 7.04 (s, 1H), 7.01 (d, *J*: 8.0 Hz, 1H), 6.88 (d, *J*: 8.0 Hz, 1H), 5.97 (s, 1H), 2.39 (s, 3H), 2.32 (s, 3H),2.29–2.31 (m, 2H), 2.19–2.27 (m, 1H), 2.03–2.09 (m, 1H), 1.74–1.77 (m, 4H); ^{13}C-NMR (100 MHz, $CDCl_3$, ppm) δ 19.1, 20.1, 21.1, 21.6(2C), 23.4, 81.7, 126.4, 126.8, 127.3, 129.9, 131.7, 136.4, 138.8, 163.7, 173.9; IR ($CHCl_3$, cm^{-1}): 2927, 1754, 1678, 1448, 1391, 1295, 1027; HRMS (ESI): calcd for $C_{16}H_{18}O_2$ [$(M+H)^+$]: 242.1307; found: 242.1319.

2.2.9. 3-([1,1′-biphenyl]-4-yl)-4,5,6,7-tetrahydroiso benzofuran-1(3H)-one (2i)

White solid (82%), m.p 76–78°C; ^{1}H-NMR (400 MHz, $CDCl_3$, ppm) δ 7.48–7.53 (m, 4H), 7.34–7.38 (m, 2H), 7.26–7.30 (m, 1H), 7.20 (d, *J*: 8.0 Hz, 2H), 5.66 (s, 1H), 2.23–2.25 (m, 2H), 2.14–2.19 (m, 1H), 1.91–1.98 (m, 1H), 1.58–1.70 (m, 4H); ^{13}C-NMR (100 MHz, $CDCl_3$, ppm) δ 20.0, 21.5(2C), 23.2, 84.3, 126.2, 127.0, 127.1, 127.6, 127.7, 128.9, 134.0, 140.3, 142.1, 163.7, 173.8; IR ($CHCl_3$, cm^{-1}): 3056, 2921, 1754, 1662, 1463, 1301, 1242, 1037; HRMS (ESI): calcd for $C_{20}H_{18}O_2$ [$(M+H)^+$]: 290.1307; found: 290.1332.

2.2.10. 3-(4-bromophenyl)-4,5,6,7-tetrahydroiso benzofuran-1(3H)-one (2j)

White solid (92%), m.p 83–85°C; ^{1}H-NMR (400 MHz, $CDCl_3$, ppm) δ 7.47–7.50 (m, 2H), 7.07–7.09 (m, 2H), 5.64 (s, 1H), 2.26–2.29 (m, 2H), 2.18–2.23 (m, 1H), 1.88–1.94 (m, 1H), 1.61–1.76 (m, 4H); ^{13}C-NMR (100 MHz, $CDCl_3$, ppm) δ 19.9, 21.4(2C), 23.0, 83.7, 123.1, 126.3, 128.2, 132.1, 134.2, 163.4, 173.5; IR ($CHCl_3$, cm^{-1}): 3063, 2934, 2251, 2047, 1901, 1755, 1589, 1488, 1296, 1007; HRMS (ESI): calcd for $C_{14}H_{13}BrO_2$ [$(M+H)^+$]: 292.0099; found: 292.0106.

2.3. Determination of AChE/BChE enzymes activity

The spectrophotometric method, reported by Ellman et al., was used to determine the inhibitory effects of the derivatives on AChE/BChE enzymes [28]. 5,5′-dithiobis(2-nitrobenzoic) acid (DTNB) was used to evaluate the activity of the enzymes AChE and BChE. The activity of both enzymes was determined spectrophotometrically at 412 nm [29].

2.4. Molecular modeling

The crystal protein structure of AChE (Protein Data Bank [PDB] ID: 6O52) [30] and BChE retrieved from the Protein Data Bank (www.rcsb.org/) [31], was prepared using PlayMolecule PrepareProtein protocol (www.playmolecule.com/) utilizing the estimated pKa values of the titratable residues in the protein [32]. The 3D structures of all ligands were sketched using ChemSketch (www.acdlabs.com) and optimized using UCSF Chimera [33]. Docking grid files were made utilizing the cocrystal ligand binding coordinates with the help of the MGLTools 1.5.6 program. AChE (x: 5.01, y: 35.37 and z: -8.38 Å), BChE (x: 42.16, y: -17.91 and z: 42.72 Å). For both proteins, a grid box of x: 40, y: 40 and z: 40 Å dimension was used. The merging of all non-polar hydrogen atoms and the addition of gasteiger charges to all atoms were done using MGLTools 1.5.6 software. Compounds **2b** and **2h** were docked into the active site, while compounds **2i** and **2j** were docked into the apparently allosteric site of AChE using AutoDock 4.2.6 (https://autodock.scripts.edu) [34], employing Larmackian Genetic algorithm with exhaustiveness value of 10 (10 runs per ligand). The binding energy of the ligand's poses were calculated and the interaction of the best pose for each ligand with AChE and BChE was examined using Biovia DS Visualizer v4.5 (BIOVIA, CA, USA).

3. Results & discussion

3.1. Chemistry

Initial reaction condition screening was started with 2-benzoylcyclohexane-1-carboxylic acid (**1a**) using CSI as the model substrate and without acid or base catalyst at room temperature in DCM or in acetonitrile. After 3h, 3-phenyl-4,5,6,7-tetrahydroisobenzofuran-1(3H)-one (**2a**) was isolated in 32 and 37% yield respectively, (Table 1, entry 1–7). Chemical characterization of (**2a**) was approved by ^{1}H-NMR, ^{13}C-NMR, HRMS and IR. To improve the yield, optimization studies were carried out. On changing with AcOH and TFA (Table 1, entries 2–5 and 8–11), the yield of **2a** increased slightly (38 and 45%) (Table 1, entries 2–3) and, (42 and 64%) (Table 1, entries 8–9), respectively. With TfOH, **2a** increased to 73 and 87% (Table 1, entries 4–10). Changing the catalyst as NEt_3,

Table 1. Condition optimization.

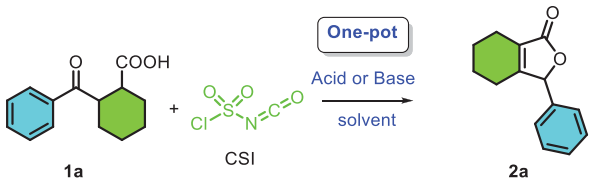

Entry	Solvents	Acid or base†	Yield‡ (%)
1	Acetonitrile	None	32
2		AcOH	38
3		TFA	45
4		TfOH	73
5		NEt_3	ND
6		TfOH and without CSI	ND
7	DCM	None	37
8		AcOH	42
9		TFA	64
10		**TfOH**	**87**
11		NEt_3	ND
12		TfOH and without CSI	ND

†Reaction conditions: **1a** (1.0 eq), CSI (1.1 eq), base or acid (cat.), solvent (10 ml).
‡ND: Not detected.
Bold Values indicates 'The best yield'.
CSI: Chlorosulfonyl isocyanate.

optimization reactions of **2a** products were not observed (Table 1, entries 5–11). Also, the optimization condition of desired product **2a** was not detected with TfOH as catalyst without CSI (Table 1, entries 6 and 12). The ideal reaction media was are ultimately determined in 87% yield, as follows, TfOH as acid catalyst in DCM at room temperature (Table 1, entry 10).

With the optimized reaction conditions in hand, transformation and the scope were carefully examined and the results are summarized in Figure 2. The reaction of 2-benzoylcyclohexane-1-carboxylic acid derivatives (*p*-methyl, *p*-ethyl, *p*-n-propyl, *p-iso*-propyl, 3,4-dimethyl, 2,5-dimethyl, 2,4-dimethyl, biphenyl and *p*-bromo) with CSI proceeded smoothly to furnish **2b** (88%), **2c** (75%), **2d** (77%), **2e** (79%), **2f** (82%), **2g** (84%), **2h** (83%), **2i** (82%), and, **2j** (92%) excellent yields in mild conditions without any metal catalyst, respectively.

A plausible mechanism for the synthesis of **2a** was suggested in light of the data. First, the carbonyl group of isocyanates and the COOH group of benzoic acid (**1a**) are attacked nucleophilically to produce carbamic anhydride (**I**). Following the protonation of the carbonyl oxygen by TfOH, carbamic anhydride (**I**) is then rearranged to carbamate (**II**) by CO_2NHSO_2Cl. Finally, intermatiated **III** undergoes isomerization to provide compound **2a** (Figure 3).

3.2. In vitro inhibition studies

Inhibition properties were investigated for benzofuranyl derivatives on AChE and BChE enzymes at a minimum of five different inhibitor doses. The IC_{50} values were determined from the activity (%) – (benzofuranyl groups) plots for each drug, defining the concentration of any compound causing 50% inhibition. The control cuvette contained no benzofuranyl groups, resulting in 100% enzyme activity. Lineweaver and Burk's curves were employed to determine inhibitor types and to calculate Ki values [35].

3.3. AChE & BChE inhibition result

Inhibitors of cholinesterase (ChE) are commonly used to treat cholinergic neurotransmission disorders [36]. Their effect on BChE and AChE is associated with the therapeutic effects of various drugs [37]. In Alzheimer's disease, downregulation of acetylcholine and butyrylcholine levels occur, which play a role in facilitating communication between nerve cells. BChE and AChE inhibitors inhibit the BChE and AChE enzymes in the brain, leading to an increase in acetylcholine and butyrylcholine levels. This can alleviate symptoms observed in Alzheimer's disease, such as memory impairment, cognitive dysfunction and overall quality of life [38].

Benzofuranyl derivatives synthesized through the reaction of 2-benzoylcyclohexan-1-carboxylic acid derivatives with CSI exhibited significantly higher AChE inhibition activity compared with standard AChE inhibitors. The benzofuranyl derivatives effectively inhibited AChE, with Ki values ranging from 0.09 ± 0.006 to 0.61 ± 0.15 μM. The Ki values for benzofuranyl derivatives (**2a–j**) and the standard compound tacrine (TAC) are summarized in Table 1. The benzofuranyl compounds (**2a–j**) strongly inhibited AChE, with Ki values ranging from 0.09 to 0.61 μM. However, these benzofuranyl derivatives (**2a–j**) exhibited almost similar inhibitory activities. Among the benzo-

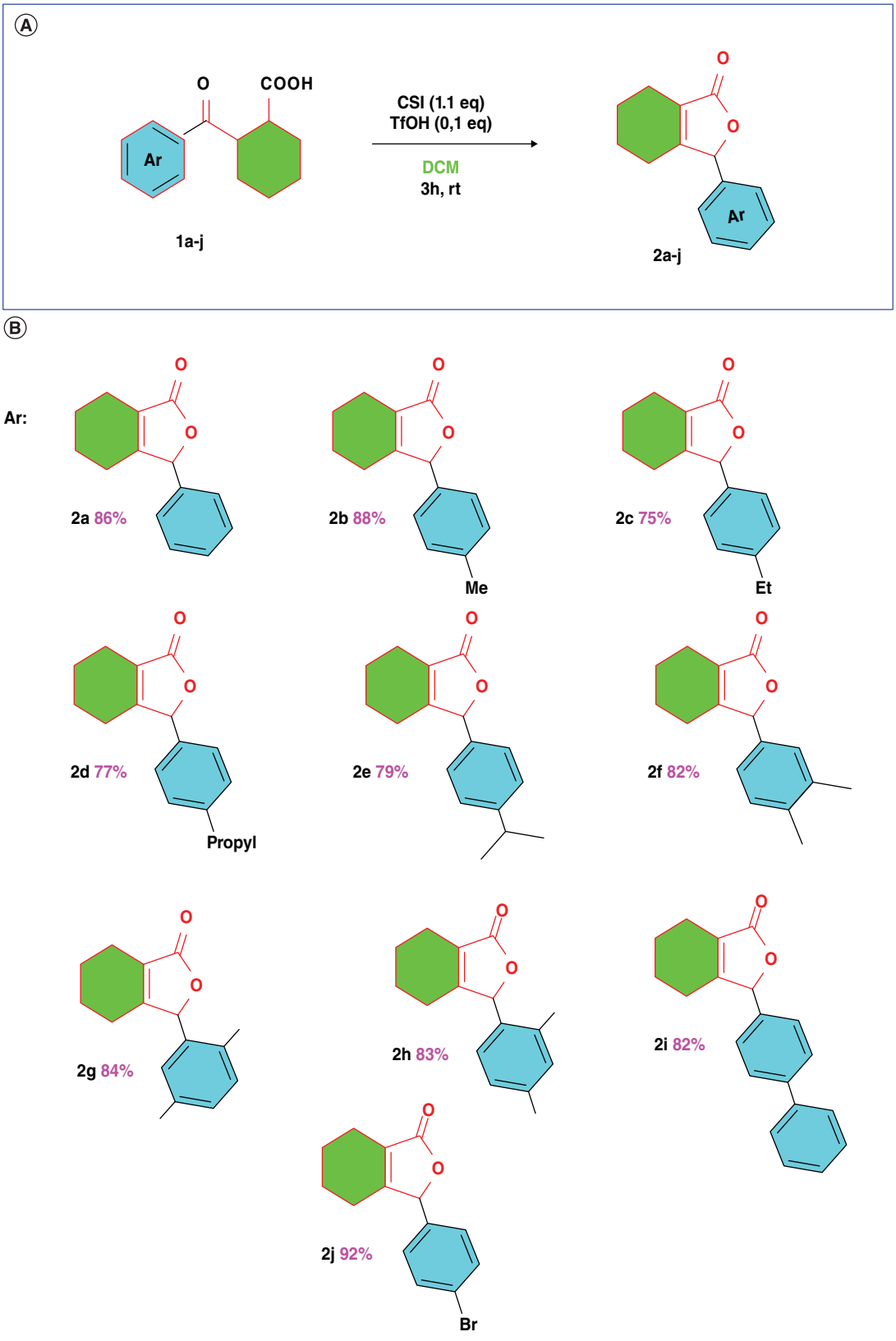

Figure 2. Substrate scope for synthesis of benzofuranyl derivatives[a,b].
[a]Reaction conditions: 2-benzoylcyclohexane-1-carboxylic acid derivatives (1.1 eq) (**1a–j**), CSI (1.1 eq), TfOH (0,1 eq), DCM (10 ml), reaction was stirred for **3h.** [b]Isolated yield.

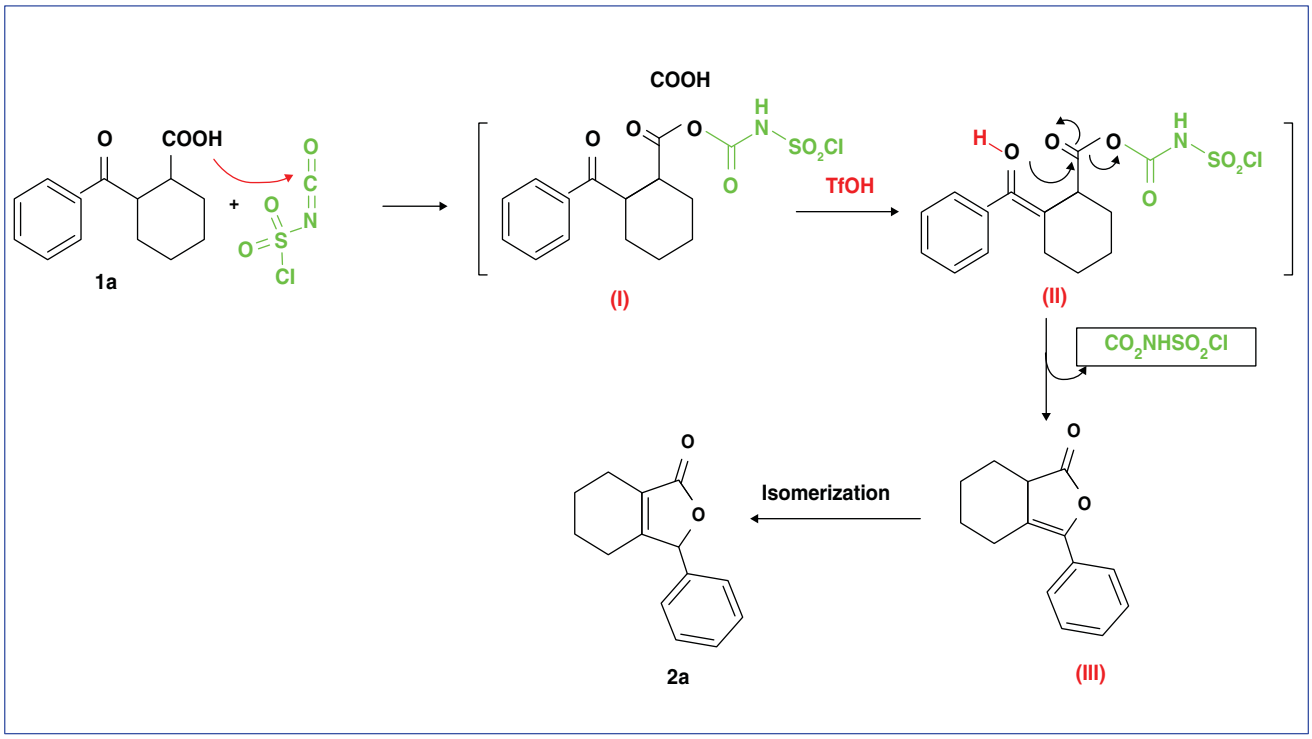

Figure 3. Proposed reaction mechanism.

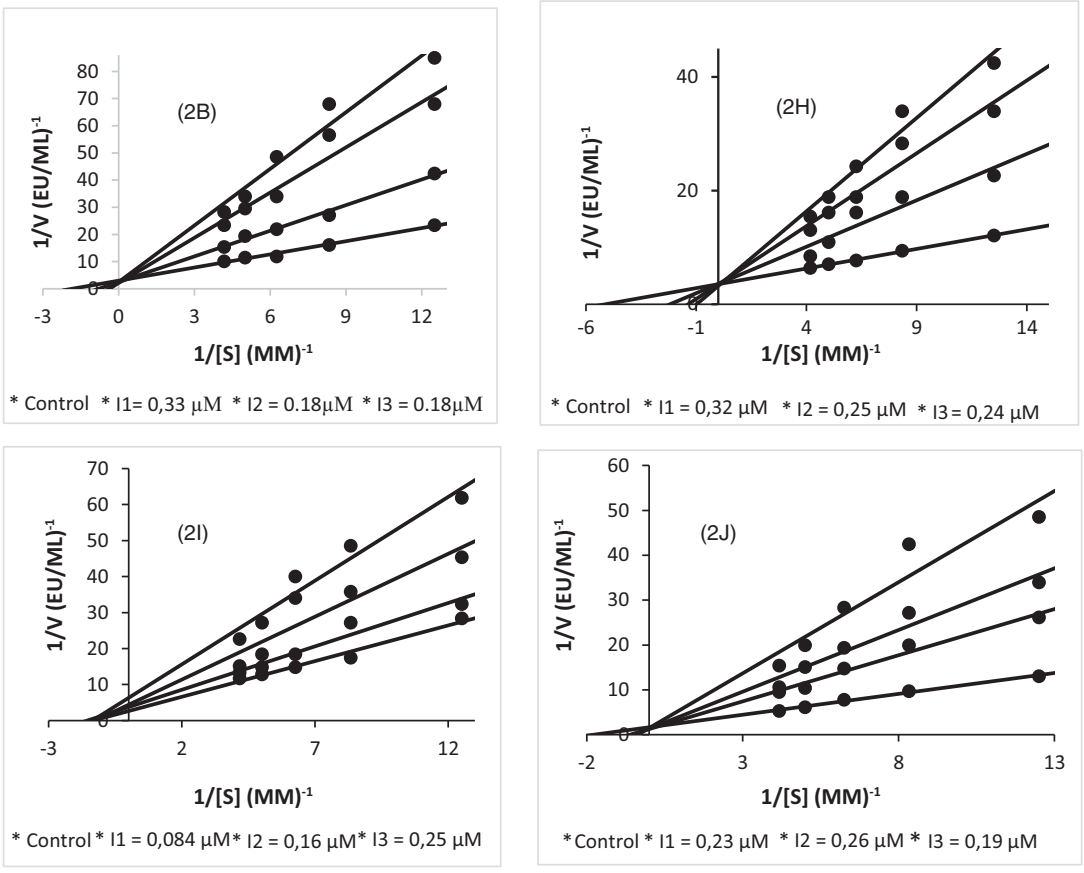

Figure 4. The Lineweaver-Burk graphs of molecules **2b**, **2h**, **2i** and **2j** demonstrating the best inhibition on AChE.

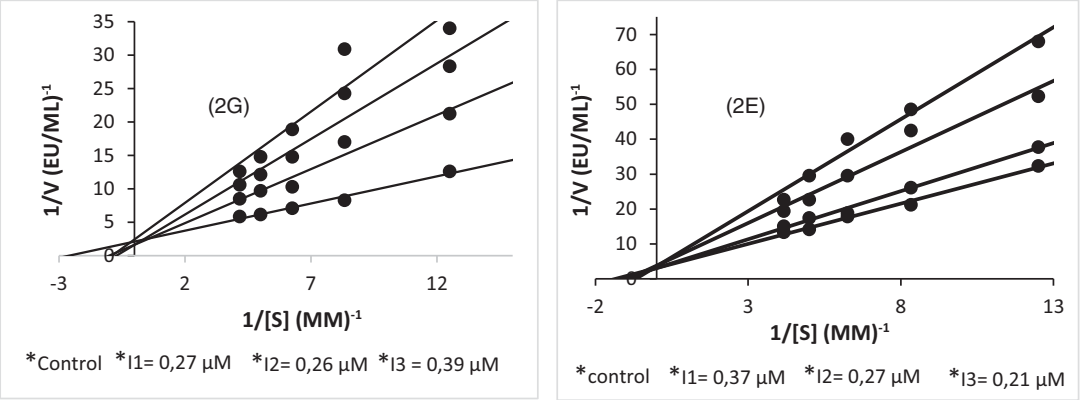

Figure 5. The Lineweaver-Burk graphs of molecules **2g** and **2e** demonstrating the best inhibition BChE.

Table 2. The enzyme inhibition results against BChE and AChE of benzofuranyl derivatives synthesized by the reaction of 2-benzoylcyclohexane-1-carboxylic acid derivatives with CSI (**2a-j**).

Compounds	IC_{50} (μM)				K_i (μM)	
	AChE	r^2	BChE	r^2	AchE	BChE
2a	4.81	0.9588	15.06	0.9569	0.61 ± 0.157	0.56 ± 0.239
2b	4.78	0.9838	14.74	0.9205	0.23 ± 0.008	0.45 ± 0.121
2c	4.95	0.9625	16.50	0.9843	0.33 ± 0.098	0.76 ± 0.240
2d	5.21	0.9474	34.65	0.9085	0.46 ± 0.055	0.66 ± 0.064
2e	4.30	0.9843	34.65	0.9085	0.32 ± 0.080	0.28 ± 0.080
2f	4.38	0.9887	33.00	0.9772	0.31 ± 0.091	0.32 ± 0.060
2g	4.25	0.9403	31.50	0.9827	0.27 ± 0.078	0.31 ± 0.071
2h	3.51	0.9384	33.00	0.9739	0.24 ± 0.072	0.41 ± 0.105
2i	4.12	0.9843	33.00	0.9085	0.009 ± 0.006	0.43 ± 0.071
2j	3.26	0.9569	14.74	0.9085	0.23 ± 0.031	1.60 ± 0.807
TAC†	3.74	0.9557	3.74	0.9757	6,19 ± 2.20	1.31 ± 2.30

†Tacrine (TAC) was used as a control for AChE and BChE enzymes.

Table 3. Binding propensity of the synthetic compounds against AChE and BChE.

Compounds	Binding energy (kcal/mol)		Mode of inhibition	
	AChE	BChE	Competitive	Uncompetitive
2b	-6.71	-5.89	AChE	BChE
2h	-6.45	-5.51	AChE	BChE
2i	-8.13	-8.98	BChE	AChE
2j	-7.79	-8.74	BChE	AChE

furanyl derivatives, **2b**, **2h**, **2i** and **2j** effectively inhibited AChE, while **2g**, **2e** and **2f** inhibited BChE strongly. (Figures 4 & 5) The most effective compound against AChE was **2j**, with Ki values of 0.009 ± 0.006 μM. The inhibition values for AChE were examined in the following order: TAC (3.74 μM, r2: 0.9557) < **2h** (3.51 μM, r2: 0.9384) < **2j** (3.26 μM, r2: 0.9569). As shown in Table 1, the benzofuranyl derivatives (**2a–j**) inhibited BChE, with Ki values ranging from 14.74 ± 0.9085 to 34.65 ± 0.9085 μM (Tables 2 & 3).

3.4. Molecular docking

Crystallographic studies based on various kinetic or calorimetric measurements have demonstrated that the active site of both cholinesterase enzymes includes ester and anionic subsites, catalytic converters and acetylcholine binding sites. The active site is formed by three catalytic residues: Glu, Ser and His. In the treatment of Alzheimer's disease, certain compounds inhibit BChE and AChE, thereby increasing ACh levels in synapses. Drug groups such as galantamine and donepezil are currently used as AChE inhibitors in clinical practice [39–41]. Our results indicate that compound **2i** was approximately 300-times much stronger AChE inhibitor compared with TAC. For AChE, **2a**, **2d**, **2e**, **2i** and **2j** exhibited uncompetitive inhibition, while **2b**, **2h**, **2f**, **2g** and **2c** showed competitive inhibition. For BChE, **2a**, **2b**, **2h** and **2c** demonstrated uncompetitive inhibition, whereas **2f**, **2g**, **2d**, **2e**, **2i** and **2j** displayed competitive inhibition.

In this study, the binding affinity and interaction of compounds **2b**, **2h**, **2i** and **2j** against AChE and BChE

were predicted. Compounds **2b** and **2h** were considered competitive inhibitors and showed a similar binding mode to that of the cocrystal ligand in the crystal structure of AChE (PDB ID: 6O52). On the other hand, **2i** and **2j** were treated as potential allosteric inhibitors that bound to an allosteric pocket close to the active site of AChE (Supplementary Figure S1). Compounds **2b** (Supplementary Figure S2A) and **2h** (Supplementary Figure S2B) were engaged with the active site of AChE via $\pi-\pi$ stacked interactions, hydrophobic contacts and a couple of Van der Waals interactions, with a unique H-bond formed between the carbonyl oxygen on the benzofuranyl group of **2h** and Phe295 in the active site of AChE (Supplementary Figure S2B). These interactions yielded a binding energy -6.71 kcal/mol for **2b** and -6.45 kcal/mol for **2h**. Phe295 is considered as one of the important constituents of the AChE active site, which participate in formation of the acyl pocket subsite [42]. In the case of potential allosteric inhibitors, **2i** and **2j** demonstrated common interactions comprising 2H-bonds, a couple of hydrophobic contacts and Van der Waals interactions, with π–cation found to be unique to **2i** (Supplementary Figure S1A) and π–anion interaction present in **2j** (Supplementary Figure S1B). In particular, the 2H-bonds formed between the benzofuranyl group of **2i** and Arg521 and Lys332 may be critical for inhibiting the activity of AChE (Supplementary Figure S3A). Similarly, **2j** formed 2H-bonds with Arg433 and Lys332 in the allosteric site of AChE via its benzofuranyl group (Supplementary Figure S3B). Compounds **2i** and **2j** were predicted to have binding energy -8.13 and -7.79 kcal/mol, respectively. In the case of the BChE complex with **2i**, two hydrogen bonds with Ala199; four hydrophobic interactions with Pro285, Leu286, Ala328 and Phe398; as well as a few Van der Waals interactions that strengthened the binding (Supplementary Figure S2A). Ala328 is a catalytically essential residue whose mutation affects the activity of BChE [43]. Similarly, compound **2j** formed two hydrogen bonds with the backbone of Gly177 and Ala99 via the benzofuranyl fragment; π–sigma and $\pi-\pi$ stacking interactions with Trp231 and Phe398, respectively, and a few Van der Waals interactions (Supplementary Figure S4B). These interactions may contribute greatly to the overall binding propensity of these ligands, reflected in the binding energy -8.98 and -8.74 kcal/mol for **2i** and **2j**, respectively. The interaction of **2b** and **2h** with allosteric pocket was rather interesting; the benzofuranyl group on both **2b** and **2h** was involved in the formation of two key 2H-bonds with Lys323 and Asn504 in the allosteric pocket of BChE (Supplementary Figure S5A & B), with respective binding energies -5.89 and -5.51 kcal/mol. Taken together, these interactions may account for the inhibitory activity of the compounds against the AChE and BChE.

4. Conclusion

In this study, a simple, efficient and one-step novel method was developed for the synthesis of benzofuranyl derivatives using CSI from 2-benzoylcyclohexane-1-carboxylic acid derivatives, and they were obtained in good yields. This method offers advantages such as a short reaction time, environmentally friendly conditions without the need for metals and mild reaction conditions. Additionally, the compounds were examined for BChE and AChE inhibition.

Molecular docking is widely used in pharmaceutical research and development to predict the binding mode of a ligand to a receptor. In this study, the inhibitory effects of benzofuranyl derivatives on AChE and BChE enzymes were investigated, and molecular docking was applied to examine the binding propensity and interactions of the most effective molecules, particularly **2b**, **2h**, **2i** and **2j** against AChE and BChE. It was observed that **2i** and **2j** exhibited high binding affinity and interactions. As a result of these investigations, it has been demonstrated that some of the benzofuranyl derivatives exhibit significantly higher inhibition on AChE and BChE compared with TAC molecules.

Alzheimer's is a complicated neurological illness with no effective treatment currently available. Drugs like TAC and similar ones can alleviate the symptoms of Alzheimer's disease, but their ability to halt or reverse the progression of the disease is limited. In comparison to drugs used for the treatment of Alzheimer's disease, such as TAC and similar ones, benzofuranyl derivatives, especially molecules like **2b**, **2h**, **2i** and **2j**, may be considered more effective and promising drug candidates as inhibitors for AChE and BChE enzymes. Consequently, these new compounds have the potential to exert a greater impact on the treatment of various diseases, including Alzheimer's disease and neurological disorders. This method can be highly practical and beneficial for the synthesis of benzofuranyl derivatives in pharmaceutical and industrial applications.

Summary points

- Highly effective one-pot synthesis of novel benzofuranyl derivatives.
- Inhibitory potentials and molecular docking of synthesized novel benzofuranyl derivatives were investigated.
- Kinetic studies were conducted for benzofuranyl derivatives with AChE and BChE.
- IC_{50} and Ki values were determined with AChE and BChE.
- The inhibition types of the inhibitors were determined.
- The most effective inhibitors were identified as **2i** for AChE and **2e** for BChE.

Financial disclosure

The authors have no other relevant affiliations or financial involvement with any organization or entity with a financial interest in or financial conflict with the subject matter or materials discussed in the manuscript apart from those disclosed.

Competing interests disclosure

The authors have no competing interests or relevant affiliations with any organization or entity with the subject matter or materials discussed in the manuscript. This includes employment, consultancies, honoraria, stock ownership or options, expert testimony, grants or patents received or pending, or royalties.

Writing disclosure

No writing assistance was utilized in the production of this manuscript.

Ethical conduct of research

The authors state that they have obtained appropriate institutional review board approval or have followed the principles outlined in the Declaration of Helsinki for all human or animal experimental investigations.

ORCID

Ufuk Atmaca https://orcid.org/0000-0002-5598-0443

References

Papers of special note have been highlighted as: • of interest; •• of considerable interest

1. Massoulié J, Pezzementi L, Bon S, Krejci E, Vallette FM. Molecular and cellular biology of cholinesterases. Prog Neurobiol. 1993;31:911. doi:10.1016/0301-0082(93)90040-Y
   •• Describes recent developments in cholinesterases.
2. Puopolo T, Liu C, Ma H, et al. Inhibitory effects of cannabinoids on acetylcholinesterase and butyrylcholinesterase enzyme activities. Med Cannabis Cannabinoids. 2022;5:1:85–94. doi:10.1159/000524086
3. Kucukoglu K, Gul Hİ, Taslimi P, et al. Investigation of inhibitory properties of some hydrazone compounds on hCA I, hCA II and AChE enzymes. Bioorg Chem. 2019;86:316–321. doi:10.1016/j.bioorg.2019.02.008
4. Jasiecki J, Wasąg B. Butyrylcholinesterase protein ends in the pathogenesis of Alzheimer's disease could BCHE genotyping be helpful in Alzheimer's therapy?. Biomolecules. 2019;9:10:592. doi:10.3390/biom9100592
5. Ağırgöl BA, Yılmaz U, İşleten F, et al. Serum bütirilkolinesteraz aktivitesinin ameliyat öncesi anksiyete ve lipit düzeyleriyle ilişkisi. Turk J Biochem. 2008;33:1:9–13.
6. Karaytuğ MO, Balcı N, Türkan F, et al. Piperazine derivatives with potent drug moiety as efficient acetylcholinesterase, butyrylcholinesterase, and glutathione S-transferase inhibitors. Biochem Mol Toxicol. 2022;37(2):e23259. doi:10.1002/jbt.23259
7. Mushtaq G, Greig NH, Khan JA, et al. Status of acetylcholinesterase and butyrylcholinesterase in Alzheimer's disease and Type 2 diabetes mellitus. CNS Neurol Disord Drug Targets. 2014;13(8):1432–1439. doi:10.2174/1871527313666141023141545
8. Özil M, Balaydın HT, Şentürk M. Synthesis of 5-methyl-2,4-dihydro-3H-1,2,4-triazole-3-one's aryl Schiff base derivatives and investigation of carbonic anhydrase and cholinesterase (AChE, BuChE) inhibitory properties. Bioorg Chem. 2019;86:705–713. doi:10.1016/j.bioorg.2019.02.045
9. Chen Z, Huang J, Yang S, et al. Role of cholinergic signaling in Alzheimer's disease. Molecules. 2022;27(6):1816. doi:10.3390/molecules27061816
10. Küçükoğlu K, Gül Hİ, Taslimi P, et al. Supuran CT, investigation of inhibitory properties of some hydrazone compounds on hCA I, hCA II and AChE enzymes. Bioorg Chem. 2019;86:316–321. doi:10.1016/j.bioorg.2019.02.008
11. Karuppiah V, Sun W, Li Z. Chapter 13: natural products of actinobacteria derived from marine organisms. Stud Nat Prod Chem. 2016;48:417–446. doi:10.1016/B978-0-444-63602-7.00013-8
    • Describes recent developments in Benzofuranyl groups.
12. Nguyen SS, Ferreira AJ, Long ZG, et al. Butenolide synthesis from functionalized cyclopropenones. Org Lett. 2019;21:8695–8699. doi:10.1021/acs.orglett.9b03298
13. Csende F. Comparative intramolecular dehydrative lactonization of 4-oxocarboxylic acids. Arkivoc. 2006;4:174–180. doi:10.3998/ark.5550190.0007.615
14. Nallasivam JL, Fernandes RA. A concise synthesis of ()-incrustoporin and its analogues by Pd-catalyzed Suzuki-Miyaura coupling from γ-Vinyl-γ-butyrolactone. ChemistrySelect. 2016;1:5137–5140. doi:10.1002/slct.201601379
15. Roach JS, LeBlanc P, Lewis NI, et al. Characterization of a dispiroketal spirolide subclass from *Alexandrium ostenfeldii*. J Nat Prod. 2009;72:1237–1240. doi:10.1021/np800795q
16. Huang SX, Yang LB, Xiao WL, et al. Novel highly oxygenated nortriterpenoids with unusual skeletons isolated from *Schisandra chinensis*. Chem Eur J. 2007;13:4816–4822. doi:10.1002/chem.200700346
17. Wang YZ, Tang CP, Dien PH, et al. Alkaloids from the roots of Stemona saxorum. J Nat Prod. 2007;70:1356–1359. doi:10.1021/np070099o
18. Fraga BM. Natural sesquiterpenoids. Nat Prod Rep. 2002;19:650–672. doi:10.1039/b108977n
19. Crossthwaite AJ, Bigot A, Camblin P, et al. The invertebrate pharmacology of insecticides acting at nicotinic acetylcholine receptors. J Pestic Sci. 2017;42(3):67–83. doi:10.1584/jpestics.D17-019
20. Seki T, Satake M, Mackenzie L, et al. A new marine toxin of unprecedented structure isolated from New Zealand oysters and the dinoflagellate, Gymnodinium sp. Tetrahedron Lett. 1995;36:7093–7096. doi:10.1016/0040-4039(95)01434-J
21. Cho CS, Kim JU, Choi HJ. Synthesis of alkyl 2,5-dihydro-5-oxofuran-2-carboxylates via palladium-catalyzed carbonylative cyclization of β-bromovinyl aldehydes in alcohols. J Organomet Chem. 2008;693:3677–3680. doi:10.1016/j.jorganchem.2008.09.014
    • Describes recent developments in Benzofuranyl groups.

22. Lee HK, Cho CS. Palladium-catalyzed carbonylative cyclizationof 3-bromoallyl alcohols leading to furan-2(5H)-ones. Appl Organometal Chem. 2012;26(8):406–409. doi:10.1002/aoc.2864
• **Describes recent developments in Benzofuranyl groups.**
23. Atmaca U. Efficient and one-pot synthesis of novel sulfamates from carboxylic acids. Tetrahedron. 2019;75(34):130467. doi:10.1016/j.tet.2019.130467
• **Describes recent developments in chlorosulfonyl isocyanate.**
24. Atmaca U. A novel approach for the synthesis of β-keto esters: one-pot reaction of carboxylic acids with chlorosulfonyl isocyanate. Arkivoc. 2020;6:220–227. doi:10.24820/ark.5550190.p011.209
25. Atmaca U, Aksoy M, Öztekin A. A safe alternative synthesis of primary carbamates from alcohols; in vitro and in silico assessments as an alternative acetylcholinesterase inhibitors. Biomol Struct Dyn. 2022;41(17):8191–8200. doi:10.1080/07391102.2022.2134209
26. Mahmoodi NO, Salehpour M. Direct synthesis of γ-substituted phthalides by cyclization of benzyl radicals generated from o-(Arylmethyl)benzoic acids. Russ J Org Chem. 2003;39(12):1760–1763. doi:10.1023/B:RUJO.0000019740.66204.fa
27. Sut S, Dall'Acqua S, Zengin G, et al. Novel signposts on the road from natural sources to pharmaceutical applications: a combinative approach between LC-DAD-MS and offline LC-NMR for the biochemical characterization of two hypericum species (*H. montbretii* and *H. origanifolium*). Plants. 2023;12(3):648. doi:10.3390/plants12030648
28. Ellman GL, Courtney D, Andres V, et al. A new and rapid colorimetric determination of acetylcholinesterase activity. Biochem Pharmacol. 1961;7:88–95. doi:10.1016/0006-2952(61)90145-9
29. Turhan K, Pektaş B, Türkan F, et al. Novel benzo[b]xanthene derivatives: bismuth (III) triflate-catalyzed one-pot synthesis, characterization, and acetylcholinesterase, glutathione S-transferase, and butyrylcholinesterase inhibitory properties. Arch Pharm. 2020;353(8):e2000030. doi:10.1002/ardp.202000030
30. Gerlits O, Ho KY, Cheng X, et al. A new crystal form of human acetylcholinesterase for exploratory room-temperature crystallography studies. Chem-Biol. 2019;309:108698. doi:10.1016/j.cbi.2019.06.011
31. Kurumbail RG, Stevens AM, Gierse JK, et al. Structural basis for selective inhibition of cyclooxygenase-2 by anti-inflammatory agents. Nat. 1996;384(6610):644–648. doi:10.1038/384644a0
32. Martínez-Rosell G, Giorgino T, De Fabritiis G. PlayMolecule ProteinPrepare: a web application for protein preparation for molecular dynamics simulations. J Chem Inf Model. 2017;57(7):1511–1516. doi:10.1021/acs.jcim.7b00190
33. Pettersen EF, Goddard TD, Huang CC, et al. UCSF Chimera-A visualization system for exploratory research and analysis. J Comput Chem. 2004;25(13):1605–1612. doi:10.1002/jcc.20084
34. Morris GM, Huey R, Lindstrom W, et al. AutoDock4 and AutoDockTools4: automated docking with selective receptor flexibility. J Comput Chem. 2009;30(16):2785–2791. doi:10.1002/jcc.21256
35. Lineweaver H, Burk D. The determination of enzyme dissociation constants. J Am Chem Soc. 1934;56(3):658–666. doi:10.1021/ja01318a036
36. Küçükoğlu K, Gül Hİ, Taslimi P, et al. Investigation of inhibitory properties of some hydrazone compounds on hCA I, hCA II and AChE enzymes. Bioorg Chem. 2019;86:316–321. doi:10.1016/j.bioorg.2019.02.008
37. Tokalı FS, Taslimi P, Usanmaz H, et al. Synthesis, characterization, biological activity and molecular docking studies of novel Schiff bases derived from thiosemicarbazide. Biochemical and computational approach. J Mol Struct. 2021;1231:129666. doi:10.1016/j.molstruc.2020.129666
38. Kuzu B, Tan M, Taslimi P, et al. Mono- or di-substituted imidazole derivatives for inhibition of acetylcholine and butyrylcholine esterases. Bioorg Chem. 2019;86:187–196. doi:10.1016/j.bioorg.2019.01.044
39. Taslimi P, Turhan K, Türkan F, et al. Cholinesterases, α-glycosidase, and carbonic anhydrase inhibition properties of 1H-Pyrazolo[1,2-b]phthalazine-5,10-dione derivatives: synthetic analogues for the treatment of Alzheimer's disease and diabetes mellitus. Bioorg Chem. 2020;97:103647. doi:10.1016/j.bioorg.2020.103647
40. SiteMap. New York, NY: Schrödinger, LLC; 2020. www.schrodinger.com/citations/
41. Gumpeny RS. Acetylcholinesterase inhibitors (galantamine, rivastigmine, and donepezil). NeuroPsychopharmacotherapy. 2022;2709–2721. doi:10.1007/978-3-319-56015-1_418-1
42. Kaplan D, Ordentlich A, Barak D, et al. Does "butyrylization" of acetylcholinesterase through substitution of the six divergent aromatic amino acids in the active center gorge generate an enzyme mimic of butyrylcholinesterase? Biochem. 2001;40(25):7433–7445. doi:10.1021/bi010181x
43. Lushchekina S, Nemukhin A, Varfolomeev S, et al. Understanding the non-catalytic behavior of human butyrylcholinesterase silent variants: comparison of wild-type enzyme, catalytically active Ala328Cys mutant, and silent Ala328Asp variant. Chem-Biol Interact. 2016;259:223–232. doi:10.1016/j.cbi.2016.04.007